4 Search for $K\pi$-atoms

Y. Allkofer, C. Amsler, A. Benelli[5], S. Horikawa, C. Regenfus, and J. Rochet

In collaboration with: Basel, Bern, Bucarest, CERN, Dubna, Frascati, IHEP-Protvino, KEK, Kyoto, Moscow, Prague, Santiago, Tokyo and Trieste

(DIRAC-II Collaboration)

The $K^+\pi^-$-atom is a hydrogen-like non-relativistic system of a K^+ and a π^- bound by the Coulomb force. The binding energy of the 1s level is 2.9 keV. The atomic level is broadened and shifted by the overlap of the pion and kaon wave functions. The atom is unstable and decays into $K^0\pi^0$. Such atoms have not been observed so far, but $\pi^+\pi^-$ atoms were studied by the DIRAC Collaboration at CERN (1). The lifetime of the 1s level is related to the difference $|a_1 - a_3|$ between the $K\pi$ S-wave scattering lengths a_1 and a_3 corresponding to the isospin 1/2 and 3/2 states, respectively.

A measurement of the scattering lengths is important for chiral perturbation theories (ChPT). In contrast to $\pi^+\pi^-$-atoms, the $K\pi$-scattering length probes ChPT extended to s-quarks in the limit where the masses of the u-, d- and s-quarks vanish. The scattering lengths can be obtained by extrapolation to zero energy from the isospin 1/2 and 3/2 S-wave phase shifts, however with substantial uncertainties due to the lack of good low energy $K\pi$-scattering data. The extrapolations from the various scattering measurements disagree by large factors: measurements of a_1 vary between 0.17 and 0.34 m_π^{-1}, those of a_3 between –0.07 and –0.14 m_π^{-1}. The scattering lengths were also computed from dispersion relations using scattering data, assuming analytical continuation, unitarity and crossing symmetry (2):

$$\begin{aligned} a_1 &= \quad 0.224 \pm 0.022 \quad \mathrm{m}_\pi^{-1} \\ a_3 &= -0.0448 \pm 0.0077 \quad \mathrm{m}_\pi^{-1}. \end{aligned}$$

However, there are inconsistencies below 1 GeV/c (2). Assuming the above values one predicts a mean life $\tau \sim 3.7$ fs for the $K\pi$-atom. Note that a 20% measurement error in the lifetime leads to a 10% error in $|a_1 - a_3|$. Details on the physics motivations can be found in our 2005 annual report.

In DIRAC-II (3) our group provides the aerogel Čerenkov counters and the heavy gas system for kaon detection. Kaons and pions are produced by the 24 GeV/c PS proton beam on target, typically a 100 μm thick nickel foil (4). The emerging particles are analyzed in a double-arm magnetic spectrometer measuring the momentum vectors of two oppositely charged hadrons (Fig. 4.1). The dissociated kaon and pion from $K\pi$-atoms emerge behind the target with a very small relative momentum $Q < 3$ MeV/c. $K^+\pi^-$-atoms, once produced, move forward and annihilate into $K^0\pi^0$, are being excited or ionize in the target. Since annihilation, excitation and ionization are competing processes, one can determine the mean life by measuring the (calculable) breakup probability in the target.

Detecting Čerenkov radiation from kaons in the DIRAC-II momentum range between 4 and 8 GeV/c requires a transparent medium with a refractive index of typically $n = 1.015$. This can be achieved with aerogel. However, the suppression of fast protons at small angles with respect to the primary beam line requires an even smaller refractive index of typically 1.008. Unfortunately the light yield decreases rapidly with refractive index, and hence

[5] Visitor from the University of Basel

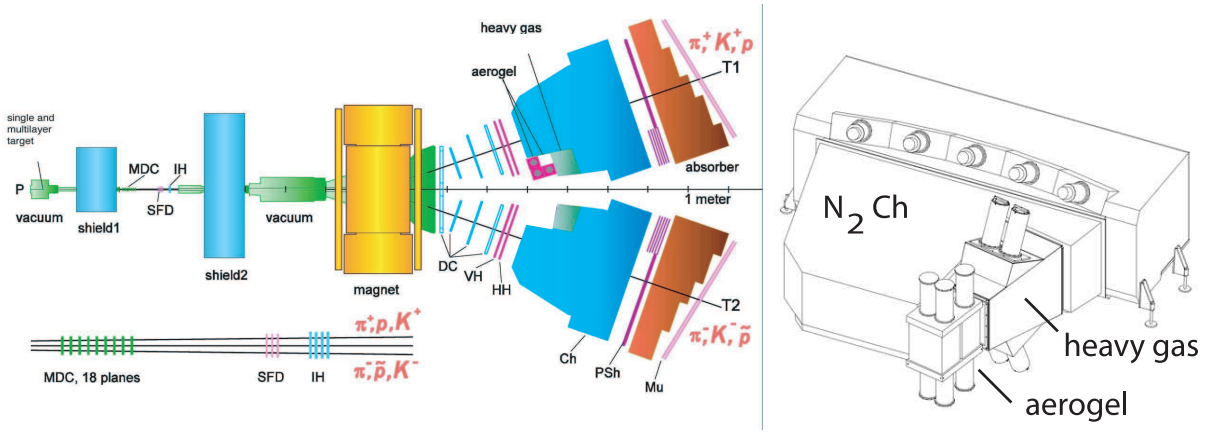

Figure 4.1: Sketch of the updated DIRAC-II spectrometer showing the locations of the Čerenkov counters to identify electrons, pions and kaons. MDC = microdrift chambers, SFD = scintillator fibre detector, IH = ionization hodoscope, DC = drift chambers, VH, HH = scintillation hodoscopes, Ch = N_2-Čerenkov counter, PSh = preshower, Mu = muon counters. Right: aerogel, heavy gas and N_2-Čerenkov counters.

R&D developments were required to achieve a reasonable light collection efficiency.

On the other hand, the faster pions and the beam contaminating electrons will also be detected by our aerogel counters. The latter are vetoed by an N_2-Cerenkov counter and the former by a heavy gas Čerenkov detector (see Fig. 4.1) for which we developed the gas distribution system. Positive kaons are detected in the left arm with the aerogel counter which also suppresses the overwhelming background from scattered protons. On the other hand, the background from antiprotons in the right arm is small so that negative kaons from $K^-\pi^+$-atoms do not need to be detected directly with an aerogel counter.

4.1 Aerogel Čerenkov-detector

In 2006 the design of the aerogel Čerenkov-counter for kaon-proton separation was finalized, the detector constructed and installed in the DIRAC-II experiment. The final detector consists of three independent modules (Fig. 4.2). Two of them have aerogel with the refractive index $n = 1.015$ for kaon-proton separation between 4 and 5.5 GeV/c (24ℓ supplied by Panasonic) and the third one has the lower index n = 1.008 for 5.5 to 8 GeV/c kaons (13ℓ purchased from the BINP/BIC Institutes in Novosibirsk).

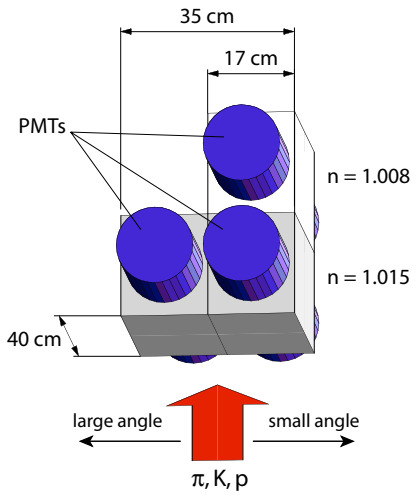

Figure 4.2: Sketch of the three aerogel counters, each read out by two (5") Photonis XP4570B photomultipliers (PMT) with UV window. Fast protons populate the small angle region with respect to the primary beam axis and are vetoed with the n = 1.008 aerogel module.

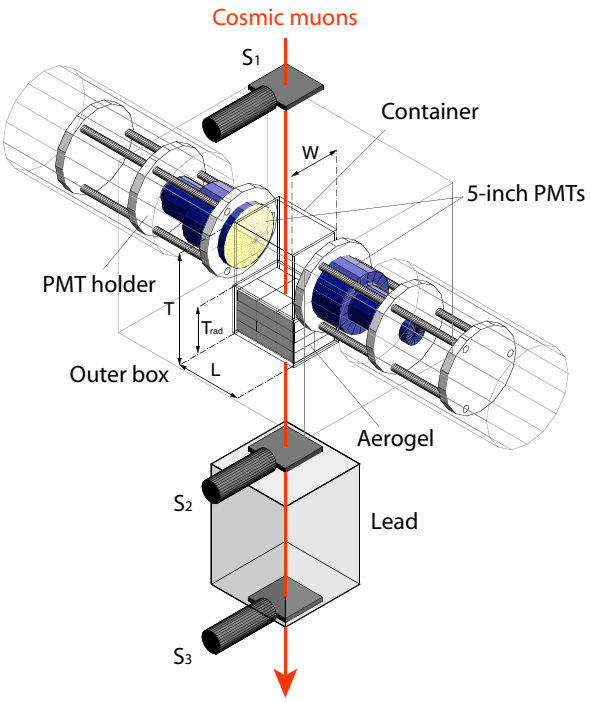

Figure 4.3: Apparatus used to measure the light yield of aerogel and the detection efficiency of Čerenkov light with cosmic rays. High energy muons are selected with the lead absorber between the scintillation counters S_2 and S_3.

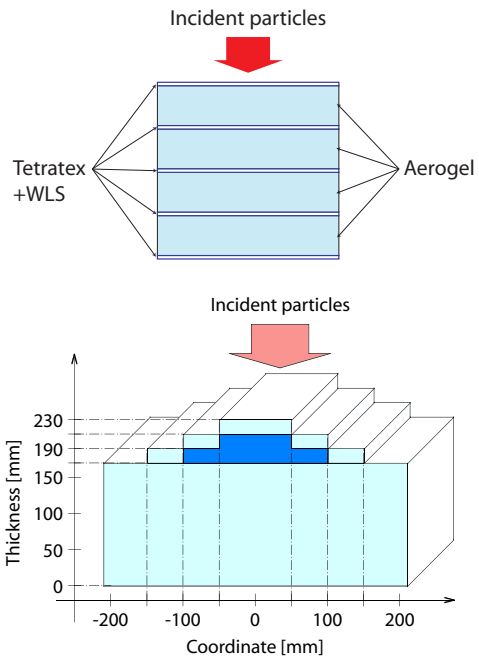

Figure 4.4: Principle of the aerogel sandwich counter (top) and pyramidal structure (bottom).

The light yield is proportional to the factor $1 - 1/\beta^2 n^2$ (where β is the kaon velocity) and therefore becomes very small for low refractive indices. On the other hand, the Čerenkov light intensity is inversely proportional to the wavelength and hence concentrated in the UV-region. We have determined the light yield for kaons using a test setup, cosmic rays and simulation (Fig. 4.3).

The light detection efficiency for kaons traversing the aerogel at equal distance (20 cm) from the two PMTs is reduced by roughly 50% compared to kaons passing near one of the photocathodes. For a 17 cm thick aerogel detector with refractive index n = 1.008 we expect between 4 and 7 photoelectrons from kaons at 7 GeV/c, depending on the impact position. However, the light absorption length depends strongly on wavelength and increases rapidly from about 10 cm at 270 nm to 3 m at 350 nm. The loss due to absorption can be compensated by using a wavelength shifter and also by increasing the radiator thickness at the center of the detector.

To compensate for the low Čerenkov light yield in the 1.008 counter and to increase the absorption length we have developed a novel sandwich design consisting of aerogel tiles interleaved with a wavelength shifter (WLS) coated reflector (such as Tetratex), as illustrated in Fig. 4.4 (top). The goal was to shift the Čerenkov UV towards blue light, thereby increasing the absorption length by two orders of magnitude, and also matching the photocathode sensitivity of the PMT. The best results were obtained with Tetratex as reflector immersed in a solution of p-terphenyl dissolved in chloroform for the WLS. This technique increased the light detection efficiency by 50%. Details on these developments can be found in our 2005 annual report and in a recent publication (5). On the other hand, the pyramidal shape compensates for the stronger absorption in the center (Fig. 4.4, bottom). The thickness of the 1.008 aerogel radiator varies from 16 to 23 cm, the thickness of

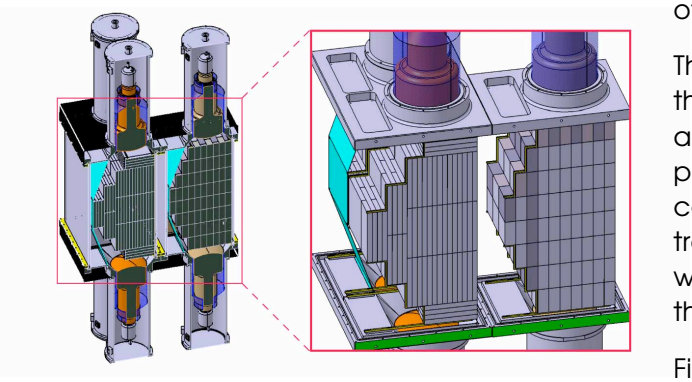

Figure 4.5:
Drawing of the final setup. The aerogel tiles are arranged in a pyramidal geometry in a steel box that also supports the housing of the PMTs and their mu-metal shields. The steel box is shielding the PMTs from the fringe field of the DIRAC dipole magnet.

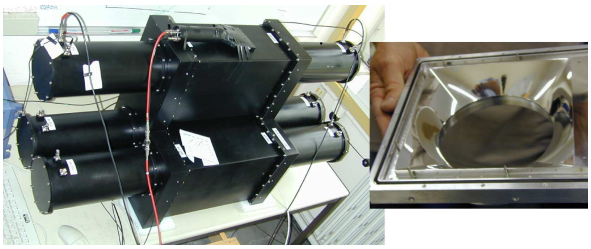

Figure 4.6:
Left: completed left arm detector.
Right: spherical mirrors to focus the light on the PMT photocathodes.

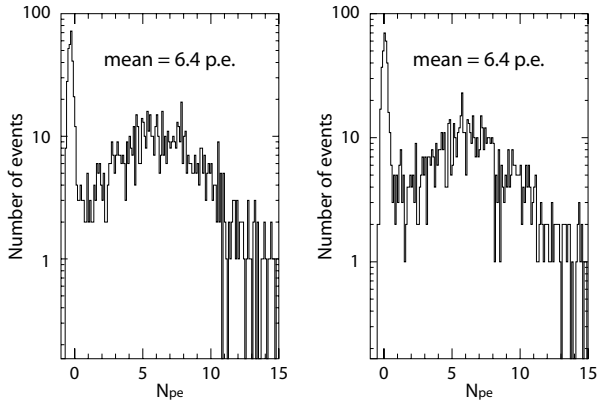

Figure 4.7:
Amplitude distribution (number of photoelectrons) for the 1.015 modules from cosmic muons passing near the PMT (left) and in the middle of the counter (right).

the 1.015 radiator from 11 to 23 cm. A drawing of the final detector is presented in Fig. 4.5.

The inner container surfaces are covered with three layers of Tetratex. The aerogel tiles are held by a steel frame covered with TiO_2 paint as diffuse reflector. The 1.008 pyramid contains 236 and the 1.015 pyramids 124 extremely fragile aerogel tiles which are held with a coarse mesh made of 250 μm thick threads.

Figure 4.6 shows the completed apparatus in our laboratory, ready for tests with cosmic ray muons, since test beams were unfortunately not available at CERN in 2005 and early 2006. The aluminium coated spherical mirrors are covered with an MgF_2 layer for which the thickness was optimized to the emission spectrum of the WLS. Apart from the mirrors most of the mechanical structure was built in the Institute's workshop. The cosmic ray test showed that the light yield did not depend significantly on the impact position (Fig. 4.7). For the 1.015 detector we obtained about 6.4 photoelectrons for cosmic muons, implying $\sim$5 photoelectrons for 4 GeV/c kaons. The performance of the 1.008 counter could not be tested with cosmic rays.

4.2 Heavy gas system

The Zurich group has also designed and built a gas recirculation system for the heavy gas Čerenkov counter. We are using C_4F_{10} (perfluorobutane) with a refractive index of 1.00137 (at 300 nm and 1 bar) to detect pions in the range 4 – 9 GeV/c, while suppressing kaons. The system (Fig. 4.8) is inspired by RICH counters used in other experiments (such as COMPASS). We purchased 30 kg of C_4F_{10} liquid from F2 Chemicals (6) Ltd., enough for four years of measurements, taking into account the unavoidable losses. C_4F_{10} liquid is first transferred from the gas bottle to the gas-liquid separation tank in the freezer (-18°C) shown in Fig. 4.9. The inner pressure is raised to $\sim$2 bar

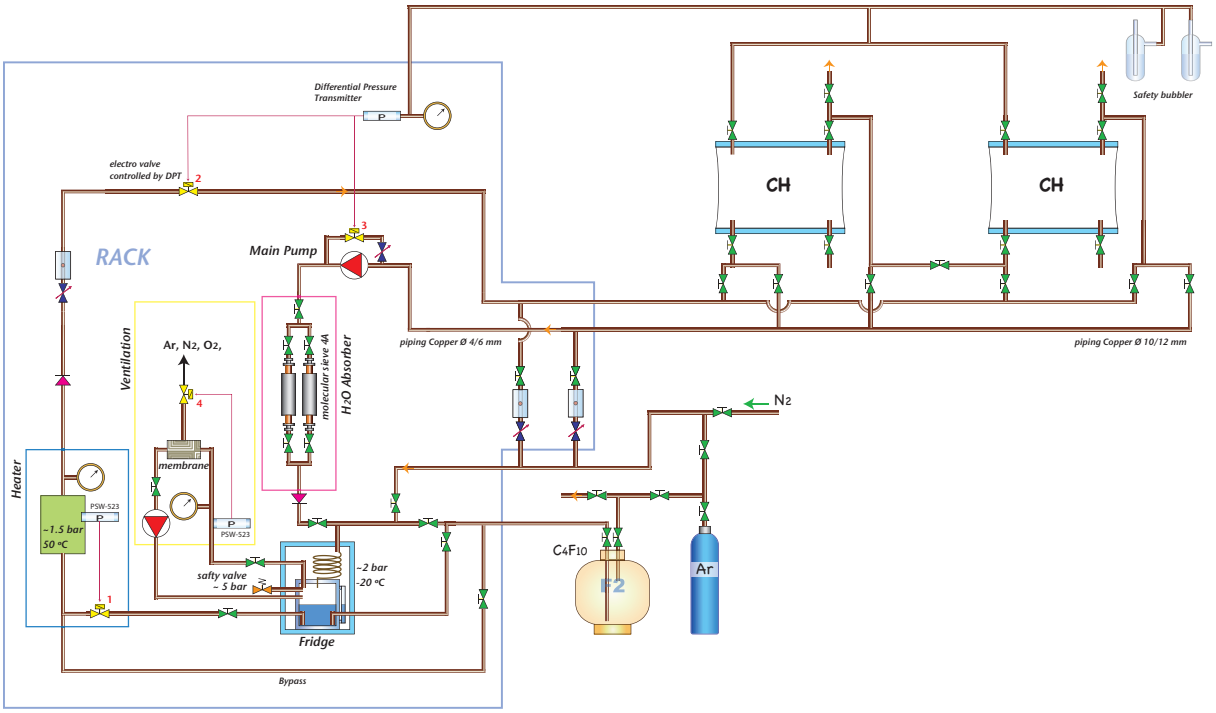

Figure 4.8: C_4F_{10} gas recirculation system. Important functions such as gas purification, pressure regulation and main circulation pump are integrated in the gas rack on the left. Valves near the two detector vessels (left and right arms of DIRAC-II) allow various circulation and recovering modes.

by the main pump to liquefy the gas, while contaminants such as nitrogen, oxygen or argon remain gaseous. This gas mixture is circulated through a hollow-fiber membrane module (7) transparent to smaller molecules.

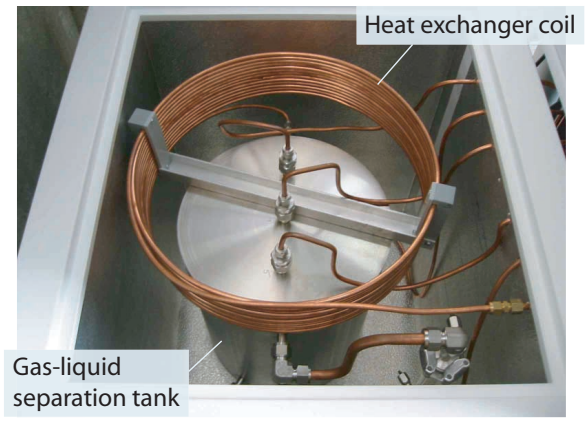

Figure 4.9: Inside the freezer: the C_4F_{10} gas returning from the detector flows through a heat exchanger coil and is liquefied before being restored in the gas-liquid separation tank.

These contaminants are thus vented to the air. The purified liquid is then transferred to the gas buffer which is heated up to 50°C. The gas returning from the detector flows through molecular sieves (4 Å) which absorb water vapor. The pressures in the separation tank and in the gas buffer are regulated using small mechanical pressure switches and electrovalves to ensure a constant flow. The tank, the buffer and the molecular sieve cylinders were constructed in our Institute's workshop.

4.3 Outlook

The aerogel detector was installed in the DIRAC-II beam line in summer 2006. The beam was turned on in late August but was soon interrupted by repeated failures of a switching magnet in the CERN primary proton beam line. This unfortunately led to the cancella-

tion of data taking in 2006. A replacement magnet will be provided for the 2007 runs. The C_4F_{10}-Čerenkov counter was built and installed with the help of our Russian collaborators in October 2006 and the assembly of the gas system was completed the following month.

Meanwhile we are developing the analysis programs. The software is being tested with data taken in 2001 to determine the lifetime of $\pi^+\pi^-$-atoms. So far some 12'000 $\pi^+\pi^-$-atoms have been observed by DIRAC. We plan to use only the detectors downstream of the dipole magnet (see Fig. 4.1). This would increase the available data sample by about a factor of 2 – 3, but presumably also increase systematic errors.

The yield of $K\pi$- atoms is expected to be about 25 $\times$ lower than for $\pi^+\pi^-$-atoms. Assuming equal acceptances and the increase in beam flux by a factor of two, this should lead to about 1'000 reconstructed $K^+\pi^-$- (and $K^-\pi^+$-) atoms during three months of data taking.

[1] B. Adeva et al. (DIRAC Collaboration), Phys. Lett. **B 619** (2005) 50.

[2] P. Büttiker, S. Descotes-Genon, B. Moussallam, Eur. Phys. J. **C 33** (2004) 409.

[3] B. Adeva et al., Addendum to DIRAC proposal, CERN - SPSC - 2004 - 009.

[4] B. Adeva et al., Nucl. Instr. and Meth. in Phys. Res. **A 515** (2003) 467.

[5] Y. Allkofer et al., submitted to Nucl. Instr. and Meth. in Phys. Res. **A**.

[6] F2 Chemicals Ltd., HTTP://WWW.FLUOROS.CO.UK/.

[7] O. Ullaland, Nucl. Instr. and Meth. in Phys. Res. **A 553** (2005) 107. [6]